https://doi.org/10.5194/egusphere-2026-2190
Preprint. Discussion started: 5 June 2026

Pre- and post-depositional processes affecting isotopic composition of seasonal alpine snowpacks — Austrian Alps

Jasper F.D. Lammers[1,2], Thomas Wagner[1], Martin Masten[1], Simon Seelig[1], Wolfgang Schöner[2], and Gerfried Winkler[1]

[1]Department of Earth Sciences, University of Graz, Graz, Austria
[2]Department of Geography and Regional Science, University of Graz, Graz, Austria

Correspondence: Jasper F.D. Lammers (jasper.lammers@uni-graz.at)

Abstract. Studying the formation and evolution of the seasonal Alpine snow pack is essential to obtain a clear picture of hydrological catchment processes during the snow season and the following melt period. In this study, three seasonal snow packs in one cirque in the Austrian Alps were monitored on a weekly interval, the snow packs were allocated in line with each other at three different elevations (1500, 1600 and 1700 m a.s.l.). We analysed the establishment of isotopic signals using atmospheric observations and a back-trajectory model. In the post-depositional analysis, we tracked individual layers over time using Dynamic Time Warping to quantify the isotopic changes and relate these changes to the layer specific temperatures, temperature gradients and isotopic gradient individually, and also a multi-linear regression approach with the combination of temperature gradient and isotopic gradients. We also tried to relate the effects of global and net radiation on the upper snow layer isotopic metamorphism. We identified that meteoric first-order isotope signals correlate strongly with cloud conditions during snow accumulation events. The second-order stable water isotope interpreter, Deuterium excess (dxs), correlates strongest to moisture origin conditions. In the post-deposition analysis we concluded that during the stable period in the snow season, trends in isotopic change are characterized by erratic week-to-week variations which always recover to the decreasing layer average. The magnitude of isotopic change increased with normalized profile depth, where the biggest fluctuations occurred at the snow-atmosphere boundary. In our analysis, week-to-week changes of the first isotopes cannot be explained solely by the snow temperature, nor the temperature gradient. However, multi-linear regression analyses of the temperature gradient and the isotopic gradient show that the temperature gradient significantly affects layer dxs changes. These dxs changes are driven by the preferential mobilization of δ^{18}O rather than δ^{2}H, contrary to classical expectations. The strong correlation between the isotopic gradient and the temporal isotopic layer metamorphism highlights diffusive homogenization as a dominant process, while temperature gradient induced vapour transport drives isotopologue differentiation. Upper layer snow isotopy is not affected by air temperature, but is affected by global radiation and net radiation. This study consolidates the idea that meteoric isotopy is shaped locally and non-locally for first- and second order isotopes, respectively. Furthermore, we highlight the coinciding processes of temperature gradient induced heterogenization of the snowpack and isotopic gradients induced homogenization.

https://doi.org/10.5194/egusphere-2026-2190
Preprint. Discussion started: 5 June 2026

1 Introduction

Seasonal snowpacks in mountain regions are major yet temporally variable freshwater reservoirs: they store water in frozen form and release it as meltwater in spring and early summer, thereby modulating river discharge, groundwater recharge, and water supply for hydropower generation and downstream populations (Wagner et al., 2017; Carroll et al., 2019; Berghuijs et al., 2014; Kulkarni et al., 2002; Stewart, 2008). The timing and magnitude of snow melt affect the availability and snow melt driven floods. Thus, continuous monitoring of snow cover is essential to hydrology and water resource management under changing climate conditions (Viviroli et al., 2007; Barnett et al., 2005; Mankin et al., 2015; Huss et al., 2017; Beria et al., 2018; Musselman et al., 2017).

Stable water isotopes — most commonly reported as δ^{18}O and δ^{2}H (expressed as permille deviation from Vienna Standard Mean Ocean Water, VSMOW) — are widely used as proxies of climate variables, hydrometeorological processes and as tracers of atmospheric source regions and hydrological pathways and processes (Stichler and Schotterer, 2000; Jasechko, 2019; Gat, 1996; Kendall and McDonnell, 1998; Aemisegger et al., 2014). The relative abundance of the two first order isotopologues relative to their lighter counterpart (i.e., ^{18}O vs. ^{16}O, and ^{2}H vs. ^{1}H) is primarily controlled by equilibrium fractionation during condensation and non-equilibrium fractionation (kinetic fractionation) during evaporation. Together, these processes generate the characteristic linear relationship between δ^{2}H and δ^{18}O, coined as the meteoric water line (Craig, 1961; Dansgaard, 1964; Gat, 1996). Globally, precipitation whose moisture originates from evaporation over oceans follows the Global Meteoric Water Line (GMWL). Because local precipitation integrates region-specific moisture sources, recycling, and evaporation conditions, the isotopic composition shifts to a Local Meteoric Water Line (LMWL). Air temperature exerts a primary control on isotopic composition along the MWL, with δ^{18}O and δ^{2}H both systematically decreasing with altitude as temperatures cool.

Deuterium-excess (dxs; $= \delta^{2}\mathrm{H} - 8 * \delta^{18}\mathrm{O}$, Dansgaard, 1964) quantifies deviations from the GMWL and serves as a second-order tracer. This second-order tracer (dxs) composition is effectively preserved during atmospheric transport between the moisture source and the location of precipitation. This allows identification of source region composition and local atmospheric conditions (Merlivat and Jouzel, 1979; Bershaw, 2018; Aemisegger et al., 2022). Since meteoric stable water isotopes are shaped by conditions and processes at both the origin and the location of precipitation, Lagrangian back-trajectory models serve as a powerful tool to identify moisture source regions, characterise atmospheric conditions, and elucidate the dominant processes shaping meteoric isotopy (Aemisegger et al., 2022; Krklec et al., 2018; Juhlke et al., 2019).

Towards understanding dominant post-depositional processes in accumulated snow, monitoring the isotopic composition is a valuable approach. The isotopic composition of snow layers can be tracked over time as a direct tracer of water molecule movement within the snowpack. Changes in snow layer isotopic composition directly reflect the direction and magnitude of internal water vapour fluxes and melt-refreeze dynamics, allowing dominant redistribution processes to be identified (Craig and Gordon, 1965; Craig, 1961; Pfahl and Sodemann, 2014; Beria et al., 2018). In addition, understanding post-depositional metamorphic processes helps in glacial paleoclimatological record interpretation. Post-depositional processes can overprint primary depositional isotopic signals, complicating paleoclimatic interpretation. Therefore, a comprehensive process frame-

https://doi.org/10.5194/egusphere-2026-2190
Preprint. Discussion started: 5 June 2026

work enables more robust deconvolution of paleoclimatic signals (Stenni et al., 2016; WAIS Divide Project Members, 2013; Harris Stuart et al., 2023).

Laboratory research has underlined the importance of sublimation, snow temperature (T_s) and stratification on post-depositional metamorphism over the course of several hours, days and weeks (Wahl et al., 2024; Schindler, 2020; Sokratov and Golubev, 2009). Isothermal snow — or snow close to this state — shows rapid compaction and liquid water mobility between the snow crystal, that causes a water drainage flux in the snowpack. Cold snow, on the other hand, promotes sublimation of water molecules from crystal surfaces with high vapour pressure and their deposition onto surfaces with lower vapour pressure. Temperature gradients (∇T_s) within the snowpack drive vapour pressure gradients, controlling the direction and magnitude of this diffusive water molecule transport (Colbeck, 1983, 1985, 1987, 1991; Pinzer and Schneebeli, 2009; Pinzer et al., 2012; Schneebeli and Sokratov, 2004). As these snow metamorphism processes are caused by sublimation and deposition processes of water vapour, changes in stable isotope composition of the snow clearly reflects those processes. Due to the fact that sublimation is a non-equilibrium fractionation process, a stronger net displacement of δ^2H compared to δ^{18}O is expected, and it is thought that a shift of layer dxs over time will appear (Sokratov and Golubev, 2009). Whether these theoretical considerations of stable isotope enrichment and depletion agree with field observations is still an open issue and require further extensive field measurements. Especially since field observations on temperature-gradient metamorphism in seasonal snow and related effects on stable isotope composition are scarce (Sinclair and Marshall, 2008), and often only focuses on the uppermost snow layer in the polar regions (Steen-Larsen et al., 2014; Ollivier et al., 2025).

Morstad et al. (2007) and Nakamura et al. (2001) identified radiation-induced near-surface snow faceting in laboratory conditions, consistent with field observations by Birkeland (1998), who also documented melt-freeze metamorphism whereby incoming solar radiation induces surface melt and subsequent refreezing in the layer below.

During clear sky nighttime conditions, the longwave net radiation can be negative, causing the snow surface temperature to drop below air temperature. Under these conditions, surface hoar can form by the net water vapour flux from the atmosphere towards the snow surface and related re-sublimation (Colbeck, 1985). Similarly, induced temperature gradients between the surface and the layer below can drive net water vapour flux towards the surface as well, again visible as surface hoar. Principally, temperature gradient metamorphism, induced by radiation, should appear as a vapour flux towards and from the surface layer, yet the linkage between radiative forced temperature gradient metamorphism and water isotopes remains largely unexplored.

Building on current knowledge gaps in pre- and post-depositional processes affecting stable isotope composition in seasonal snow, this study uses extensive field observations to characterise meteoric isotopy establishment and to identify the dominant processes altering isotopic composition after deposition in Alpine snow cover. We present weekly high vertical-resolution profiles of δ^{18}O, δ^2H and dxs throughout the mid-to-end seasonal snowpack from a field site in the Austrian-Alps, paired with continuous measurements of snow temperature and snow temperature gradients and observations of associated atmospheric conditions above the snow. By jointly evaluating (i) atmospheric conditions at the precipitation site and moisture source region, (ii) drivers of temperature gradient metamorphism (T_s and ∇T_s), and (iii) radiative induced thermal metamorphism drivers

https://doi.org/10.5194/egusphere-2026-2190
Preprint. Discussion started: 5 June 2026

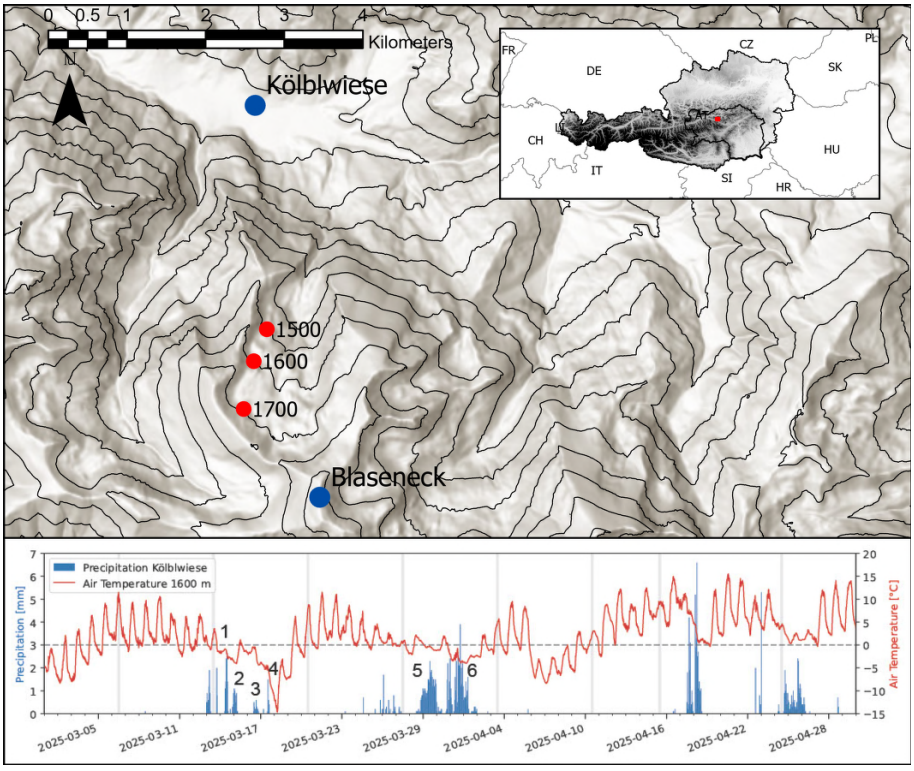

Figure 1. Overview of research area with contour lines. Snow profiles were sampled every week at the three red dots in the period from 06-03-2025 to 24-04-2025. Atmospheric data used for analyses were retrieved from valley station Kölblwiese (856 m a.s.l.) and mountain station Blaseneck (1969 m a.s.l.), both indicated with blue dots. In the part below, the time series of the air temperature at 1600 meters above sea level [°C] and precipitation [mm] are shown in red lines and blue bars respectively. The air temperature is interpolated from the temperature at the top of the mountain ridge and the temperature in the valley with an average lapse rate of 0.504°C 100 m^{-1} (similar lapse rates in the Alps shown in Rolland, 2003; Rist et al., 2020). The valley station is the nearest station with precipitation records and is therefore used. Numbers in the lower figure depict the observed snow events. Gray bars in the background denote the moments of snow sampling. Background hillshade: Esri, Geoland, Intermap, NASA, NGA, USGS

(R_{glob}, R_{net}) within a consistent stable isotope stratigraphy, we seek to quantify the driving variables establishing the isotopic signal and variables altering the isotopic signal for alpine seasonal snow.

2 Field site

Snow sampling was carried out at three locations in the Bärenkargraben cirque (from now on referred to as BK) in the Johnsbach valley in Styria, Austria (Figure 1). Snow samples were taken at three different elevations, all in line of the same aspect, but with different vegetation. All sites have a North-North-East exposure, with the Rotkogel ridge at their back. The sites are allocated at 1497, 1578, and 1694 meters above sea level, respectively. For simplicity, from now on the sites are referred to

https://doi.org/10.5194/egusphere-2026-2190
Preprint. Discussion started: 5 June 2026

their rounded off elevations of 1500, 1600 and 1700 meters. The three sites are within one kilometre of each other. Sites 1500 and 1600 are in a small clearance in a forest, while site 1700 is entirely above the forested area. Sites 1600 and 1700 are at the bottom of slopes over 30 degrees, in contrast to the area around 1500, which is more or less flat.

Solar radiation and air temperatures are continuously measured at two meteorological stations monitored as part of the WegenerNet (Fuchsberger and Kirchengast, 2023): one atop the highest peak of the catchment (Blaseneck, 1969 m a.s.l., 1.5 km from observation sites) and the other in the valley (Kölblwiese, 856 m a.s.l., 2.5 km from observation sites). Annual air temperature averages at Blaseneck and Kölblwiese are 3.1°C and 7.1°C respectively, and have average precipitation sums of 1223 mm. Air temperatures at the three field sites are derived from interpolation between the two meteorological stations using the lapse rate (seasonal average: 0.54 °C 100 m^{-1}). These air temperatures were later used for isotopic establishment analysis and post-depositional isotopic metamorphosis analysis, this is further described in the methodology chapter.

At each location, an array of thermometers was installed. Each consisting of 5 to 6 thermometers in an array of ten centimetre intervals to record snow temperatures (T_s) every 15 minutes. Because of an upward shift of the lower thermometers during installation, a gap in the sensor array near the snow-soil surface was created, meaning that no snow temperatures were recorded during the snow season near the bottom. However, this also meant that above the created sensor gap, temperatures were recorded in a higher vertical resolution. From the array of snow temperatures, the vertical temperature gradients (∇T_s) were derived.

3 Methodology

3.1 Snow sampling

To collect snow samples from multiple adjacent profiles that can be treated as a single continuous profile throughout the study period, a simple yet effective sampling strategy was applied. After sampling — just before closing the snow pit — we installed two wooden poles in the snow at the edge of the snow profile we have taken samples from. The poles stuck out of the snow so that next time we could identify the exact sampling location from last time. The poles were installed with their intersection axis perpendicular to the slope. This way, profiles were dug at the same location as last week, but only slightly further up the slope, presenting a snow profile, untouched from previous excavations and mixed refilling. We were especially careful to close the snow pits fully, to prevent any parts of the snow pack that are naturally not in contact with the atmosphere, to be covered again. We also never touched the snow upwards from the two poles, to prevent any unnatural disturbance of the snow pack. A graphical overview of the profile sampling method is presented in the Supporting Information (Figure S1).

In addition to taking core samples, we documented the snow temperature, snow crystal size and shape, and the snow wetness according to the ICSSG standards (Fierz et al., 2009).

Snow samples were taken with an aluminium cylinder (diameter: 8 cm, height: 5 cm) that was gently pushed horizontally into the snow, and carefully removed in order to preserve the snow density of the sample. Snow samples were emptied from the cylinders into Whirl-Pak® bags. To inhibit fractionation during transfer to the laboratory, any excess air was removed before the bags were sealed. These bags were weighed in the field on a spring scale and later weighed again in the laboratory of the University of Graz with a digital scale. For each sample, we measured electrical conductivity (EC) before being stored in

https://doi.org/10.5194/egusphere-2026-2190
Preprint. Discussion started: 5 June 2026

sealed opaque HDPE bottles. Samples were analysed on stable water isotopes δ^{18}O and δ^{2}H with an Elementar iso FLOW spectrometer. The resulting isotopic compositions are expressed in parts per thousand (‰) deviating from the Vienna Standard Mean Ocean Water (VSMOW). The precision of the measurements was 0.615‰ and 0.042‰ for δ^{2}H and δ^{18}O respectively. From the two first order isotopes, dxs was derived according to the Dansgaard equation (Dansgaard, 1964).

Since the accumulated snow did not visibly preserve individual snow-event layers, we could not sample one core per event. Consequently, some cores contained snow from multiple snow events. The measured isotopic composition of a core therefore represents a mixture of the contributing events rather than a single event. Using the cumulative precipitation time series, we quantified the fractional contribution of each event to each core and used these fractions as weights when relating the observed snow isotopic composition to meteorological conditions (discussed in the next paragraph). An illustrative example of two snow accumulation events contributing to a single sampling core is shown in Figure S2.

3.2 Model, data, and analyses

3.2.1 Atmospheric drivers of meteoric isotopy

To assess atmospheric drivers of meteoric stable water isotope composition at the three BK sites, we explored Pearson correlations between δ^{2}H, δ^{18}O, and dxs and atmospheric conditions at both the study site and identified moisture source regions (Aemisegger et al., 2022). For atmospheric input data for back-trajectory modelling, we used the ERA5 Reanalysis dataset (ECMWF) (Hersbach et al., 2020). ERA5 reanalysis outperforms any earlier or other reanalyses (e.g., ERA-Interim, JRA-55, MERRA-2) in terms of accuracy of temperature, wind, humidity, and precipitation fields (Graham et al., 2019; Huang et al., 2021; Hassler and Lauer, 2021). From the ERA5 data set the following variables were used at 18 atmospheric levels; three dimensional wind velocity components ($\boldsymbol{u}, \boldsymbol{v}, \boldsymbol{w}$), air temperature ($T_{air}$) and relative humidity (RH). The layers ranged from 1000 hPa to 100 hPa. At the surface level, the geopotential (W), air pressure (P_0), 2-meter temperature ($T_{2\mathrm{m}}$), and 10-meter wind components ($\boldsymbol{u_{10}}, \boldsymbol{v_{10}}, \boldsymbol{w_{10}}$) were used. In addition, cloud temperature and pressure at cloud top were derived from ERA5 as well.

We determined the trajectory the air parcel has taken before precipitating at our observation sites with HYSPLIT (Hybrid Single Particle Lagrangian Integrated Trajectory). HYSPLIT (Draxler and Hess, 1998) is an atmospheric parcel-tracing model applying an Eulerian and Lagrangian approach. For each snow event, we simulated an ensemble run of 27 individual trajectory simulations. Each of the 27 runs is initialized by slightly different conditions in order to consider the uncertainty of the simulations and allow to identify the most probably path of air parcels from the origin to the study site (Draxler and Hess, 1998).

To obtain the signal from moisture sources along the atmospheric trajectories, and not that of moisture sinks, we applied the approach of Sodemann et al. (2008). Along each trajectory, increases in specific humidity are identified as evaporative moisture uptake events, marking the geographic location of that uptake as a moisture source. The fractional contribution of each source to the total moisture carried by the air parcel at the point of precipitation is weighted by the magnitude of

https://doi.org/10.5194/egusphere-2026-2190
Preprint. Discussion started: 5 June 2026

the uptake relative to all subsequent additions, and reduced by any precipitation loss occurring between the source and the observation site. No source is ever fully excluded; even a distant or minor uptake event retains a proportional, though potentially very small, contribution to the final precipitated signal. The atmospheric conditions at each identified source region are then integrated into a single representative value through a weighted average, where each source location contributes proportionally to its fractional moisture contribution. This allows the isotopic signal of freshly deposited snow to be linked to the blended atmospheric conditions across all moisture sources along the trajectory. This methodology has also applied by Aemisegger et al. (2022); Pfahl and Sodemann (2014); Dütsch et al. (2017). To correlate source, transport and cloud formation processes with meteoric stable water isotopes, we adapted the approach by Aemisegger et al. (2022). This way, we can pinpoint establishment dynamics of meteoric stable water isotopes to; the temperature 2 meters above the surface ($T_{2\mathrm{m}}$), cloud temperature (T_c), air temperature at the moisture origin (T_{o}), cloud cooling temperature (T_{c-o}), cloud top pressure ($P_{c,top}$) and the relative humidity of the moisture origin (RH_{o}). $\mathrm{P_{c,top}}$ is used as an available and appropriate substitute for the vertical cloud structure. The cloud temperature is calculated as the specific humidity weighted temperature, therefore incorporating the distribution of water in the atmospheric column. A schematic overview of the methodology is shown in Figure S3

3.2.2 Post-depositional metamorphism

In order to track the weekly isotopic changes of individual snow layers, we applied a Dynamic Time Warping algorithm (DTW, Giorgino, 2009) on the profile time series. This algorithm measures the similarity between two temporal signals considering signal speed and spread. Through the DTW algorithm, we were able to link isotopic layers over the course of two to eight weeks, allowing us to quantify changes in layer isotopy. To maintain uniformity in post-depositional analyses, we standardized the linked layer isotopy changes in permille per day (‰ d^{-1}).

To identify which post-depositional processes shape snow isotopy over time, and how much these processes affect snow isotopy, potential drivers of snow metamorphism were statistically linked to the temporal evolution of isotopic layer compositions. Using snow thermometer arrays, we related weekly isotopic change to (i) the weekly mean snow temperature and temperature gradient ($\overline{T_{\mathrm{s,w}}}$ and $\overline{\nabla T_{\mathrm{s,w}}}$), (ii) the mean snow temperature and temperature gradient during the 24 h preceding sampling ($\overline{T_{\mathrm{s,24h}}}$ and $\overline{\nabla T_{\mathrm{s,24h}}}$), and (iii) the vertical isotopic gradient between adjacent layers during the preceding sampling interval ($\nabla_{\mathrm{iso,\,w-1}}$). $\nabla_{\mathrm{iso,\,w-1}}$ was calculated as the isotopic difference between the target layer and the adjacent layers above and below for each of the first- and second order isotope. For uniformity, ∇_{iso} is expressed in permille per centimetre (‰ cm^{-1}).

Correlations between temporal isotopic changes and drivers of these changes are expressed with Pearson r and the p-value. We identified significant correlations when $p < 0.05$ and highly significant when $p < 0.01$.

All post-depositional correlation analyses were performed during the period prior to freshet (SSP), ranging from March 6$^{\mathrm{th}}$ to April 10$^{\mathrm{th}}$ 2025. We refer to this period when less detrimental changes in isotopy as the Stable Snow Period (SSP). Snow metamorphism post-SSP are dominated by snow melt. The SSP ended when the snow profile became isothermal and moist, indicating the onset of the melt period. Since there have been too few observations on isotopic changes during the last two weeks, potential drivers of wet isotopic metamorphism are neglected in statistical analyses.

https://doi.org/10.5194/egusphere-2026-2190
Preprint. Discussion started: 5 June 2026

4 Results

4.1 Pre-deposition: Drivers of meteoric isotopy

4.1.1 Snow events

In total, we identified six snow accumulation events in which a significant amount of snow was added to the research area (lower panel Figure 1). Events 1 to 4 have all deposited snow between the second and third weekly campaign (between March 13$^{\text{th}}$ to March 20$^{\text{th}}$), and events 5 and 6 snow were deposited between the fourth and fifth weekly campaign (March 27$^{\text{th}}$ to April 3$^{\text{rd}}$).

Using the cumulative precipitation sum and the sampling depths, it became evident that the first four snow events (Figure 1) are sampled as mixed samples. Snow from snow accumulation events 1 and 2 is mixed in one core sample, as is snow from events 3 and 4 mixed in another single core.

At all elevations, δ^{18}O of the events 3+4 were -16‰, and -20‰ for events 1+2 (Figure 2). Similarly, at all elevations, the δ^{2}H and dxs values for events 1+2 are -150 and 5.3‰ respectively. δ^{2}H and dxs values for events 3+4 are slightly more spread over the elevations: at 1500, δ^{2}H and dxs were highest (-105 and 16.24 ‰ respectively), whilst at 1600 and 1700 the δ^{2}H and dxs were about -118 and 9.0 ‰.

The added snow - observed on April 3$^{\text{rd}}$ - had distinctive layers as well. The precipitated volume snow was big enough to differentiate between individual snow events from March 29$^{\text{th}}$ to April 2$^{\text{nd}}$ of precipitation. The upper layers show relatively low compositions of δ^{18}O and δ^{2}H (-11 and -85 ‰), similar values to the deepest fresh layers. However, the dxs-values of these upper layers are all relatively low compared to the other freshly deposited snow layers. In the middle of the snow pack, the highest δ^{18}O and δ^{2}H compositions were found (-9 and -62 ‰). The dxs signal of the mid-depth snow, on the other hand, was higher than the upper layers, but lower than the lower layers. The lowest fresh snow layer shows a relative abundance of δ^{2}H compared to δ^{18}O.

4.1.2 Atmospheric drivers snow isotopy

The fresh snow δ^{18}O signals show significant correlations ($p<0.05$) with T_c, T_{c-o}, and RH_{o}, and a highly significant correlation ($p<0.01$) with $P_{c,top}$ (Table 1). δ^{2}H shows significant correlations with all predictive variables and the correlation is highly significant with the cloud temperature. Pearson's r drops when T_c is subtracted from T_{o} (i.e., cloud cooling), thus, cloud cooling has a lower predictive value than that of T_c alone. Apart from RH_{o}, all variables showed positive correlations with both δ^{2}H and δ^{18}O. These first order isotopes are therefore strongly linked to local atmospheric conditions during precipitation.

The isotopic lapse rate, which is the linearly regressed slope between δ^{18}O and $T_{2\text{m}}$, is 0.429 ‰ °C^{-1}, which is slightly lower than the 0.464 and 0.53 of ‰ °C^{-1} in Jouzel et al. (1997) and Delattre et al. (2015). The relationship between δ^{18}O and origin temperature was 0.725, i.e. steeper than the aforementioned studies and results. The $T_{2\text{m}}$ – δ^{2}H relationship has a slope of 10.12 ‰ °C^{-1}, and T_{o} – δ^{2}H has a slope of 7.48 ‰ °C^{-1}, which is less steep than the local air temperature-isotope relationship.

https://doi.org/10.5194/egusphere-2026-2190
Preprint. Discussion started: 5 June 2026

Table 1. Pearson correlation for potential drivers of pre-depositional isotopic signals. Pearson correlation coefficient (r) and p is the significance level of the hypothesis. Significant p-values are highlighted in bold. Correlations are shown between the freshly deposited isotopic signals, δ^{18}O, δ^{2}H and dxs, and the air temperature 2 meters above the ground ($T_{2\mathrm{m}}$), cloud top air pressure ($P_{c,top}$), temperature at moisture origin (T_{o}), cloud temperature (T_c), the cloud cooling temperature (T_{c-o}), and relative humidity at moisture origin (RH_{o}).

	δ^{18}O		δ^{2}H		dxs	
n = 21	r	p-value	r	p-value	r	p-value
$T_{2\mathrm{m}}$	0.422	0.0569	0.518	**0.0162**	0.837	**0.0000**
$P_{c,top}$	0.550	**0.0098**	0.508	**0.0187**	-0.106	0.6473
T_{o}	0.375	0.0940	0.461	**0.0358**	0.743	**0.0001**
T_c	0.608	**0.0035**	0.610	**0.0033**	0.230	0.3154
T_{c-o}	0.548	**0.0101**	0.528	**0.0138**	0.052	0.8222
RH_{o}	-0.434	**0.0494**	-0.525	**0.0145**	-0.806	**0.0000**

dxs shows highly significant correlations with $T_{2\mathrm{m}}$, T_{o} and RH_{o}. These correlations are the most significant of all isotope - atmospheric condition relationships, and show the strongest linear correlation (r = 0.837, 0.743, and -0.806 respectively). $T_{2\mathrm{m}}$ and T_{o} have a positive relationship with dxs, while RH_{o} showed a negative relationship with dxs. For a visual overview of the data points and correlations, the reader is kindly referred to Figure S4.

4.2 Post-deposition: Drivers of snow metamorphism

4.2.1 Isotopic changes within snow profiles

The temporal variability of snow isotopy changes increased with normalized snow depth during the SSP (Figures 2 and S5). Surface layers exhibited the largest fluctuations, whereas middle and basal layers were comparatively stable, indicating that upper snowpack layers are most susceptible to post-depositional modification while deeper layer isotopy is preserved. The lowest temporal variability occurred at a normalized depth of 0.25.

In the upper layers, δ^{18}O and δ^{2}H showed a pronounced week-to-week variability, slightly increasing over the study period. dxs varied substantially without a systematic long-term trend. At the onset of melt (April 6$^{\mathrm{th}}$–15$^{\mathrm{th}}$), the upper 3–4 layers merged as the snow depth decreased, resulting in a uniform δ^{18}O composition across elevations ($-9.6‰$). This merged layer was isotopically more enriched than any of its original constituent layers, indicating that melt-induced enrichment cannot be explained by simple layer mixing alone. During the same time, dxs decreased more strongly than expected from the weighted layer averages, implying preferential mobilization of δ^{2}H relative to δ^{18}O into the liquid phase. Layers below showed increasing dxs values, consistent with isotopic fractionation during wet metamorphism.

By the second week of freshet, the snowpack had become nearly isotopically homogeneous. The weighted average δ^{18}O, δ^{2}H and dxs remained stable between over the last two sampling weeks (black dotted lines in Figure 2).

https://doi.org/10.5194/egusphere-2026-2190
Preprint. Discussion started: 5 June 2026

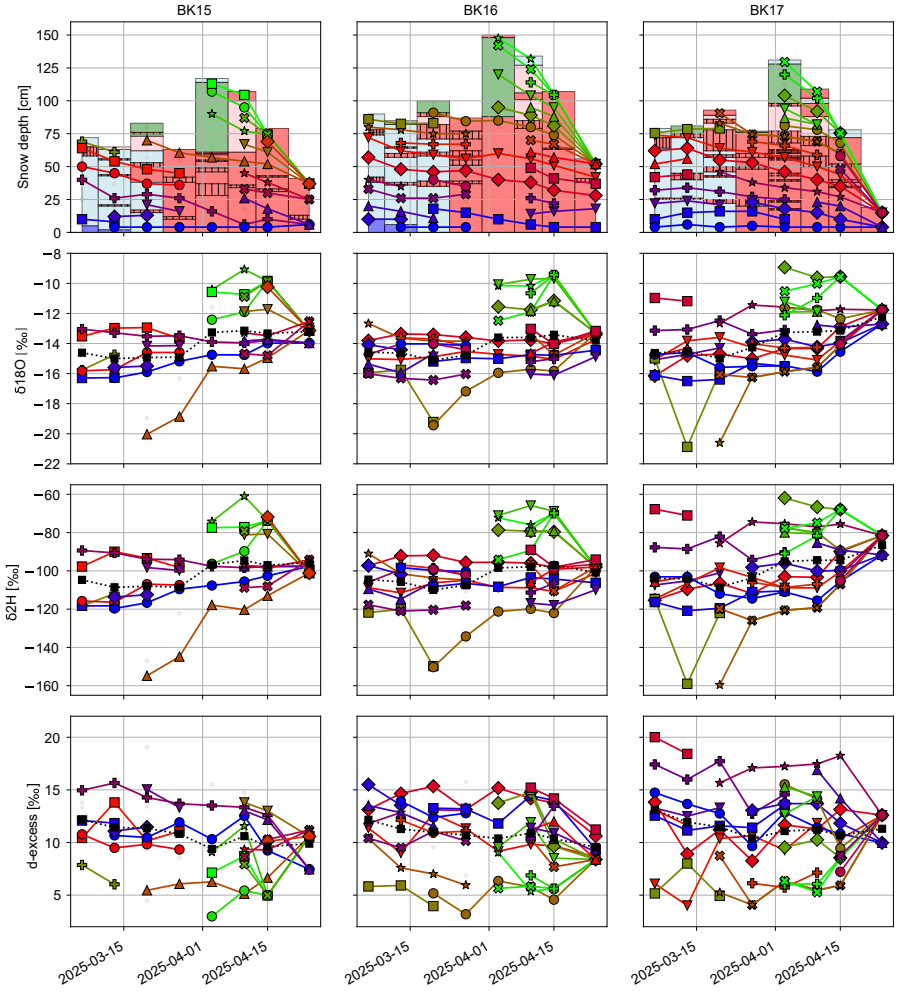

Figure 2. Time evolution of snow depth, snow layers and isotopy composition for the three snow sampling sites at 1500, 1600 and 1700 m.a.s.l. The upper figures show the depths of the taken samples, and the profile snow crystal types according to ICSSG. Colours for snow crystal types are plotted slightly translucent to make the figure more readable. The second, third and fourth row of figures show δ^{18}O, δ^{2}H, and dxs compositions of each colour- and symbol coded layers. Black dotted lines with squares represent the weighted average snow composition of these profiles.

Basal layers exhibited minimal variation in δ^{18}O throughout the SSP. Although dxs occasionally showed abrupt changes, these generally reverted to previous levels, indicating no persistent long-term trend. During freshet, basal δ^{18}O increased toward the bulk snowpack average, while dxs decreased and remained consistently below the snowpack average. In some cases, the basal dxs became lower than those of all overlying layers. This suggests relative enrichment in δ^{18}O compared to δ^{2}H in basal snow, consistent with preferential melt-out of δ^{2}H and the retention of δ^{18}O.

https://doi.org/10.5194/egusphere-2026-2190
Preprint. Discussion started: 5 June 2026

4.2.2 Snow metamorphism and snow isotopy composition

The week-to-week change of δ^{18}O, δ^{2}H does not show a correlation with the weekly average temperature of the snow, nor the temperature gradient during the preceding week or the last 24 hours prior to observation (Table 2). However, Δdxs is highly significantly correlated with the weekly temperature gradient, and even stronger correlated with the temperature gradient during the last 24 hours before observation. The predictive values of the weekly and diurnal temperature gradient on the isotopic change alone are 0.227 and 0.320 (the square of Pearson r values in Table 2).

The prevailing vertical isotopic gradient correlates most strongly with temporal isotopic change in both first- and second order isotopes. Positive correlation coefficients indicate that layers with steeper isotopic gradients undergo greater isotopic change over time, moving towards a more homogeneous profile. Specifically, the direction of isotopic change in each layer follows the prevailing local gradient, with layers that are isotopically depleted relative to their neighbours enriching and those enriched relative to their neighbours depleting over time.

Although $\overline{\nabla T_{\mathrm{s,w}}}$ alone has no predictive value for weekly isotopic changes (Table 2), its multi-linear combination with $\nabla_{\mathrm{iso,\,w-1}}$ significantly explains $\Delta\delta^{18}$O and Δdxs (Table 3). For $\Delta\delta^{18}$O, 49% of variance is explained by this combination, with both $\nabla_{\mathrm{iso,\,w-1}}$ and $\overline{\nabla T_{\mathrm{s,w}}}$ returning significant coefficients ($p = 0.049$). For Δdxs, 32% of variance is explained, though $\overline{\nabla T_{\mathrm{s,w}}}$ does not significantly predict $\Delta\delta^{2}$H (p = 0.314), suggesting that temperature gradient influence on hydrogen isotopologue transport is less direct or more variable than for oxygen. Notably, the negative temperature gradient coefficient in the Δdxs model ($\beta_{\overline{\nabla T_{\mathrm{s,w}}}}$ = -2.042), combined with the significant positive coefficient in the $\Delta\delta^{18}$O model (β = 0.315) and the non-significant response of $\Delta\delta^{2}$H ($\beta = 2.467$, $p = 0.314$), indicates that dxs reduction under positive temperature gradients is driven by displacement of ^{18}O towards colder layers, rather than by preferential ^{2}H mobilization as conventionally expected.

Considering the aforementioned results, we can identify two major processes that affect the isotopic change of snow layers: (i) Fickian diffusive processes homogenize stark isotopic gradients in the snow, and (ii) snow temperature gradients create preferential displacement of ^{18}O over ^{2}H, causing differentiation of the isotopes in the snow pack.

Shown in Table 4, the metamorphism of the first-order isotopes in the upper layer correlates positively with weekly global radiation ($\overline{R_{glob,w}}$) and net radiation 24 hours prior to sampling ($\overline{R_{net,24h}}$). This positive relationship indicates the enrichment of heavy isotopologues from solar radiation induced thermal gradients at the snow surface. Under sublimation, kinetic fractionation would be expected to cause a decrease in dxs. However, dxs shows no significant correlation with global or net radiation (Table 4), suggesting that sublimation-related kinetic fractionation was not the dominant radiation-thermal gradient induced process during the SSP. Given the limited sample size (n = 15), this result should be interpreted with caution. The results suggests equilibrium fractionation dominating under the observed conditions. Radiation induced equilibrium fractionation is consistent with melt–refreeze processes, in which lighter isotopologues are preferentially lost to the liquid phase, leaving the residual snow enriched in δ^{18}O and δ^{2}H.

https://doi.org/10.5194/egusphere-2026-2190
Preprint. Discussion started: 5 June 2026

Table 2. Pearson correlation statistics between potential drivers of post-depositional isotopic change and the observed isotopic change of individual snow layers during the SSP. Pearson correlation coefficient (r) and p denote the correlation strength and significance level respectively. Significant p-values are highlighted in bold. $\overline{T_{\mathrm{s}}}$ and $\overline{T_{\mathrm{s,24h}}}$ are the weekly average snow layer temperature and the 24-hour average temperature prior to sampling, respectively. $\overline{\nabla T_{\mathrm{s}}}$ and $\overline{\nabla T_{\mathrm{s,24h}}}$ are the weekly average temperature gradient and the 24-hour average temperature gradient of the snow layer, respectively. $\nabla_{\mathrm{iso,\,w-1}}$ is the vertical isotopic gradient from the previous sampling interval.

	$\Delta\delta^{18}$O		$\Delta\delta^{2}$H		Δdxs		
	r	p-value	r	p-value	r	p-value	n
$\overline{T_{\mathrm{s,w}}}$	0.086	0.6407	0.114	0.5356	0.142	0.4376	32
$\overline{\nabla T_{\mathrm{s,w}}}$	0.133	0.4668	-0.039	0.8311	-0.476	**0.0060**	32
$\overline{T_{\mathrm{s,24h}}}$	-0.013	0.9449	-0.071	0.6980	-0.297	0.0987	32
$\overline{\nabla T_{\mathrm{s,24h}}}$	0.029	0.8760	-0.083	0.6535	-0.563	**0.0008**	32
$\nabla_{\mathrm{iso,\,w-1}}$	0.510	**0.0000**	0.685	**0.0000**	0.353	**0.0000**	142

Table 3. Pearson correlation statistics of multi-linear regression models predicting weekly isotopic change ($\Delta\delta^{18}$O, $\Delta\delta^{2}$H, and Δdxs) from the prevailing vertical isotopic gradient ($\nabla_{\mathrm{iso,\,w-1}}$) and the mean weekly temperature gradient ($\overline{\nabla T_{\mathrm{s,w}}}$). Pearson correlations (r and p-value) for each component and the corresponding coefficients (β) are presented together with the multi-linear regression performance score R^2. Significant p-values are highlighted in bold.

	$\nabla_{\mathrm{iso,\,w-1}}$		$\overline{\nabla T_{\mathrm{s,w}}}$		
n = 37	β	p-value	β	p-value	R^2
$\Delta\delta^{18}$O	0.541	**0.000**	0.315	**0.049**	0.494
$\Delta\delta^{2}$H	0.293	**0.000**	2.467	0.314	0.387
Δdxs	0.306	**0.011**	-2.042	**0.004**	0.324

5 Discussion

Previous studies focus on high-frequency isotopic snow metamorphism over short periods (Wahl et al., 2024; Sokratov and Golubev, 2009), on long-term snow metamorphism with sparse temporal coverage (Sinclair and Marshall, 2008; Anderson et al., 2016; Pu et al., 2020), or on spatially inconsistent sampling strategies that do not follow the same profile over time, leaving the direct layer-scale links between metamorphic drivers and isotopic change poorly constrained (Carroll et al., 2022; Noor et al., 2023). Here, we bridge this gap by monitoring seasonal snowpack isotopy evolution at weekly resolution. Despite sublimation and related processes acting on minute-to-hour timescales (Wahl et al., 2024), we observed isotopic changes of similar magnitude, indicating that weekly sampling captures the cumulative impact of short-term metamorphic processes. This highlights weekly monitoring as a cost-effective strategy to quantify seasonal snow isotopic evolution. So, although weekly

https://doi.org/10.5194/egusphere-2026-2190
Preprint. Discussion started: 5 June 2026

Table 4. Pearson correlation statistics between upper snow layer isotopic change and radiation variables. Radiation variables include global radiation (R_{glob}) and net radiation (R_{net}) over the past week and 24 hours. Significant p-values are highlighted in bold.

	$\Delta\delta^{18}$O		$\Delta\delta^{2}$H		Δdxs	
n = 15	r	p-value	r	p-value	r	p-value
$\overline{R_{glob,w}}$	0.525	**0.045**	0.549	**0.034**	0.477	0.072
$\overline{R_{glob,24h}}$	-0.294	0.287	-0.170	0.545	0.369	0.175
$\overline{R_{net,w}}$	0.557	**0.031**	0.483	0.068	0.047	0.868
$\overline{R_{net,24h}}$	0.621	**0.013**	0.589	**0.021**	0.284	0.305

sampling cannot resolve individual short-term events, it integrates their net isotopic effect at the layer scale.

Our research highlights local and non-local processes influencing the isotopic snow signature, and post-depositional isotopic evolution of an alpine seasonal snow pack. By using a back-trajectory model and regressing the modelled local and non-local meteorological conditions with precipitated isotopic signals, we were able to identify that first order isotopes (δ^{18}O and δ^{2}H) are primarily shaped locally. Cloud temperature (T_c) and cloud top air pressure ($P_{c,top}$) were identified to strongly shape meteoric isotopy. These variables more or less reflect the same principle, higher clouds are colder. The dependence of first order isotopes on T_c has been observed in isotopic lapse rates (Zhu et al., 2018; Beria et al., 2018; Kern et al., 2014) and isotopic seasonality (Feng et al., 2009; Kern et al., 2014), and is a product of Rayleigh fractionation.

dxs, on the other hand, has primarily non-local origins. The inverse relationship between dxs and relative humidity at the moisture-source (RH_o) reflects the Craig-Gordon framework (Craig and Gordon, 1965). In air masses with high relative humidity, the effect of kinetic fractionation on moisture uptake from terrestrial or oceanic sources is suppressed. In contrast, dry air masses are diffusion-limited, enhancing kinetic fractionation leading to a stronger relative enrichment of δ^{2}H compared to δ^{18}O. The strong relationship between dxs and moisture origin temperature (T_o) is ambiguous. Although T_o and RH_o are strongly anticorrelated (*r = -0.623*, *p = 0.003*), it is RH_o that directly governs kinetic fractionation during moisture uptake. Temperature primarily modulates RH, and therefore acts more as an indirect proxy shaping dxs rather than a direct driver of isotopic fractionation itself (Aemisegger and Sjölte, 2018).

The high correlations of dxs with RH_o reinforce the established understanding that dxs is preserved from moisture origin and the moisture origin processes that shape it in the first place (Craig, 1961; Pfahl and Sodemann, 2014; Beria et al., 2018; Aemisegger et al., 2022; Uemura et al., 2008; Steen-Larsen et al., 2014; Fujita and Abe, 2006). The even stronger positive correlation of dxs with T_{2m} was previously not observed to our understanding. We argue that the T_{2m} – dxs relationship is an artifact of the original air mass temperature. The positive linear correlation between T_{2m} and T_o (r = 0.708, p = 0.000) supports

https://doi.org/10.5194/egusphere-2026-2190
Preprint. Discussion started: 5 June 2026

this idea. So, even though T_{2m} appears to have the strongest link with dxs, it acts as a secondary proxy, indirectly reflecting moisture origin conditions rather than directly governing isotopic fractionation.

Negative correlations between dxs and T_{2m} have previously been observed. Natali et al. (2022) illustrated that event precipitation dxs shows no correlation with the air temperature during summer in Italy. Monthly averaging did show a significant negative dxs – T_{2m} correlation. Fujita and Abe (2006) showed negative correlations of dxs with ambient air temperature at Dome Fuji, Antarctica (Table 5). Natali et al. (2022) hypothesized that the negative monthly T_{2m} – meteoric dxs relationship can be attributed to sub-cloud droplet evaporation in summer at lower topographic locations. However, these physics cannot explain the negative relationship for Antarctic station Dome Fuji. Fujita and Abe (2006) hypothesized that RH at moisture origin shaped the dxs signal, but showed no evidence. This discrepancy in explanations and the usage of local meteorology as proxies, highlights the entanglement of processes that interplay, and stresses the need for a uniform methodology that could quantify underlying processes individually.

To interpret observed dxs signals more robustly, we propose that a two-step framework is required. First, back-trajectory modelling should be used to constrain the dxs signal imprinted at moisture origin and locally established first order isotope signals (Dütsch et al., 2017; Sodemann et al., 2008; Sodemann and Stohl, 2009; Aemisegger et al., 2022). Second, deviations between the predicted source dxs and the observed precipitation signal should be analysed to quantify post-source modifications, such as sub-cloud evaporation, re-evaporation, mixing, and catchment-scale fractionation processes. Constraining these processes will allow for a clearer separation of source signals from atmospheric and hydrological overprinting. This framework is essential for improving the interpretation of precipitation isotope data, disentangling input signals from catchment storage and mixing effects in spring discharge records, and refining paleoclimate reconstructions from ice-core archives (Jouzel et al., 1997; Merlivat and Jouzel, 1979).

However, before we reach that point, it should be noted that continental moisture recycling introduces an additional layer of isotopic modification, shaped by soil evaporation, vegetation transpiration, and boundary-layer mixing. Soil–plant–atmosphere isotope interactions are highly dynamic and species- and ecosystem-dependent (Sprenger et al., 2016; Dubbert and Werner, 2018). Therefore, more continental-atmosphere isotope observations will help disentangle the complex superposition of recycled and advected moisture signals.

Unfortunately, the extent of our thermometer array was not sufficient to record snow temperatures of basal layers. Therefore, no potential thermally induced isotopic changes could have been linked at the lowest part of the snow profile. However, as the observed temperature gradients decreased with normalized depth over the recorded extent, one could assume that the temperatures and temperature gradients were less extreme, deeper in the snow. This was observed by Dafflon et al. (2022), they found a drop in temperature gradients with depth over the entire seasonal snow pack in the East River watershed (Colorado). Similarly, Filippa et al. (2014) observed over 67 years of snow temperature profiles, that the bottom layer shows continuously high snow temperatures and low temperature gradients. During our sampling campaign, manually recorded snow temperatures underlined this process. In addition, the largest temperature gradients and isotopic changes were recorded closest to the snow-atmosphere boundary (Figure 2). This indicates that upper snowpack layers are most susceptible to post-depositional isotopic

https://doi.org/10.5194/egusphere-2026-2190
Preprint. Discussion started: 5 June 2026

Table 5. dxs - T_{2m} correlations in literature and our study.

Study	p-value	r
Natali et al. (2022) event	> 0.05	0.025
Natali et al. (2022) monthly	< 0.001	-0.492
Fujita and Abe (2006)	< 0.0001	-0.717
Our study	< 0.0001	0.837

Note: (Natali et al., 2022) used Spearman's rank coefficient. Furthermore, we took the average correlation of the 5 stations correlations in Natali et al. (2022). With the available data of Fujita and Abe (2006) we calculated the Pearson Correlation.

modification. Deeper layers, by contrast, largely retain the isotopic composition acquired at the time of burial, once temperature gradients become too weak to drive further diffusion. This raises the question of what critical temperature gradient magnitude or burial depth marks the transition from active isotopic modification to signal preservation — a threshold that, once constrained, could significantly improve the interpretation of isotopic stratigraphies in seasonal Alpine snow.

Our observations indicate that the weekly changes of δ^{18}O and δ^{2}H are largely insensitive to the snow temperature or temperature gradient alone, whereas Δdxs is strongly correlated with both weekly and diurnal temperature gradients. The prevailing isotopic gradient is the strongest predictor of both first- and second-order isotopic changes, with larger isotopic gradients driving stronger vertical homogenization. In a multiple regression model, both the isotopic and temperature gradients significantly influence Δdxs and $\Delta\delta^{18}$O, demonstrating that isotopic gradients induced diffusion and temperature gradient induced vapour fluxes coincide.

Water vapour diffuses through the pore space of the snow cover along isotopic gradients, producing vertical homogenization across all isotopic species. The temperature gradient additionally drives directional vapour fluxes that produce a reduction in dxs. However, contrary to the classical expectation of preferential ^{2}H displacement under non-equilibrium fractionation (Craig and Gordon, 1965), our statistic results indicate that this dxs reduction is driven by the mobilization of ^{18}O towards colder layers, while ^{2}H transport remains statistically indistinguishable from zero at the layer scale. This suggests that under field conditions, temperature gradient metamorphism acts on δ^{18}O and δ^{2}H asymmetrically, a finding that challenges the prevailing sublimation-based framing and warrants further investigation. The positive effect of the dxs gradient on Δdxs further indicates that kinetic fractionation is superimposed on this isotopic gradient-driven diffusion, consistent with previous observations (Harris Stuart et al., 2023) and with theoretical expectations from dry-snow metamorphism models (Touzeau et al., 2018). Overall, our results support the concept that snow isotopic metamorphism during the SSP is governed by the interplay of isotopic and temperature gradients.

https://doi.org/10.5194/egusphere-2026-2190
Preprint. Discussion started: 5 June 2026

Melt-freeze metamorphism requires careful interpretation. Increased global and net radiation likely enhanced near-surface snow temperatures and promoted melt–refreeze cycles and/or enhanced vapour exchange at the snow–air interface. The positive correlations between radiation and $\delta^{18}O$ and $\delta^{2}H$, combined with the absence of a significant dxs response, suggest that equilibrium fractionation dominated and that sublimation-related kinetic fractionation was negligible during the observation period. This is consistent with previous studies reporting isotopic enrichment of residual snow during melt processes, while sublimation typically leads to a decrease in dxs.

Radiation absorbed at the snow surface generates near-surface warming, steepening local temperature gradients and potentially inducing melt-freeze metamorphism under sufficient energy input. Because snow temperature is inherently a function of radiative fluxes, temperature gradient metamorphism and melt-freeze metamorphism cannot be fully separated in field observations. Part of the isotopic signal attributed to radiation may therefore reflect temperature gradient-driven vapour transport, and near-surface temperature gradients recorded during the SSP may partly be radiation-induced. The current analysis reflects the net effect of both processes acting simultaneously rather than their individual contributions.

Results from radiation induced melt-freeze metamorphism should be considered with caution because the three field sites differed substantially in forest cover and surrounding topography, whereas radiation data were obtained from nearby meteorological stations located in open terrain. Canopy shading, terrain-induced horizon obstruction, and differences in surface albedo likely caused site-specific deviations between measured and actual radiation at the snow surface, contributing to noise in the regression analysis.

Additionally, regression relationships differed between individual sites and the pooled dataset. With only five temporal observations per site, site-specific regressions have limited statistical power. However, the site-discrepancies suggest spatial heterogeneity in radiation-driven isotopic metamorphism, reflecting differences in canopy cover, aspect, and snowpack microclimate.

These findings highlight the importance of canopy structure and microtopography in controlling snow isotopic evolution, implying that isotope-based snow process studies in forested terrain require co-located radiation measurements.

6 Conclusions

In this study, we consolidate the idea that origin, atmospheric transport, and cloud processes shape the isotopic composition of precipitation. The identification of cloud temperature as the primary control on first-order meteoric isotopy, and moisture origin relative humidity as the primary control on dxs, provides a basis for improving isotope-enabled hydrological mixing models and for refining paleoclimate reconstructions from snow and ice archives.

The most important meteorological variable embedding its signal in the initial first-order snow isotopy is the cloud temperature, shaping the isotopy through Rayleigh fractionation. The meteoric dxs signal is shaped by the origin relative humidity. This clearly shows that, unlike first order isotopes, precipitation dxs is unaffected by local meteorology and the signal is formed at the air mass origin. In line with the Craig-Gordon framework, high relative humidity at moisture sources inhibits kinetic

https://doi.org/10.5194/egusphere-2026-2190
Preprint. Discussion started: 5 June 2026

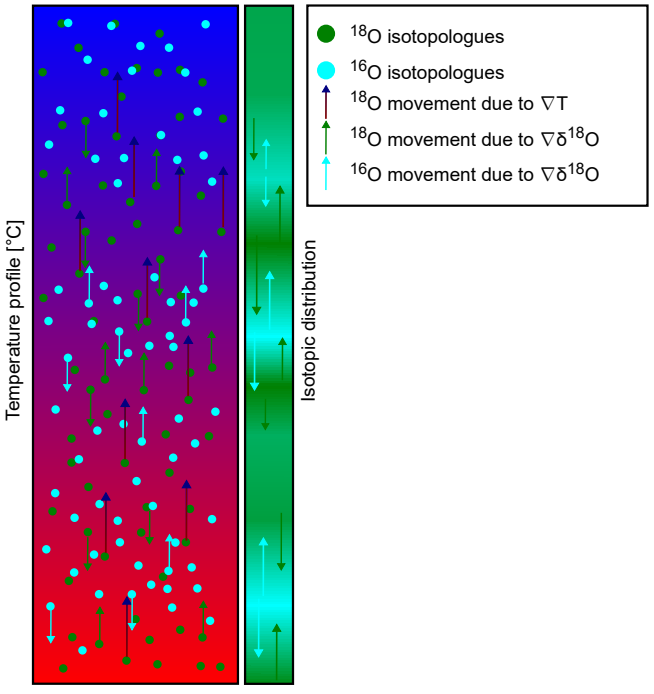

Figure 3. Conceptual illustration of the two competing isotopic redistribution mechanisms active during the stable snow period. The temperature gradient within the snowpack is presented in the left column with the heavy (green) and light (cyan) oxygen isotopologue distributed on top of it. The isotopic distribution of these isotopologues is presented for clarity on the profile next to it. Red-blue arrows in the figure illustrate the temperature gradient directed movement of ^{18}O, the green and blue arrows illustrate the Fickian diffusion of the ^{18}O and ^{16}O isotopologues respectively.

fractionation, while at low relative humidity, kinetic fractionation embeds discrepancies in the linear δ^{18}O – δ^{2}H relationship.

During the stable snow period (SSP), i.e., the period when the snowpack remains relatively dry and largely unaffected by bulk liquid redistribution, stable water isotope redistribution is governed by an interplay of two competing transport mechanisms: directed vapour transport driven by temperature gradients, analogous to advection, and Fickian diffusion driven by isotopic gradients acting to homogenize the snowpack. These co-occurring processes are illustrated in Figure 3. From the negative dxs – thermal gradient relationship, combined with the significant temperature gradient response of $\Delta\delta^{18}$O and the non-significant response of $\Delta\delta^{2}$H, we conclude that temperature gradient driven vapour transport preferentially mobilizes ^{18}O towards colder layers. This asymmetric isotopologue response challenges the classical expectation of preferential ^{2}H displacement under non-equilibrium fractionation, and suggests that the reduction in dxs under positive temperature gradients is driven by ^{18}O redistribution rather than ^{2}H mobilization. The isotopic gradient simultaneously drives diffusive homogenization of the snowpack, acting in parallel with temperature gradient induced advection.

https://doi.org/10.5194/egusphere-2026-2190
Preprint. Discussion started: 5 June 2026

In terms of radiation affecting the upper layer of snow, the upper layer isotopy is affected strongest by the weekly average global radiation and the net radiation 24 hours before sampling. Solar radiation does not induce significant kinetic fractionation and is therefore hypothesized to drive melt–refreeze processes, with lighter isotopologues preferentially lost to the liquid phase percolating into the snowpack.

During the melt period, liquid redistribution causes rapid homogenization of the snowpack. The bulk snowpack isotopy does not change distinctively, indicating equal melt-out from all layers without any strong kinetic fractionation at the end of the seasonal snow.

Future research should aim to explore higher-resolution temporal observations and expand the spatial scope to better capture short-term processes and regional variability in isotopic snowpack dynamics. In particular, high-resolution co-located measurements of snow isotopy, snow temperatures, and radiation will be essential to formally separate radiation-induced from temperature gradient-induced metamorphism, and to further investigate the asymmetric mobilization of ^{18}O and ^{2}H under natural temperature gradient conditions.

Data availability. All discussed observations from Bärenkargraben and the meteorological stations are available at: https://doi.org/10.4211/hs.cf8ad9c275464c0faaf9fe4a3ada05f7 (Lammers, 2025). This includes the HYSPLIT analyses.

Author contributions. JL, TW, MM and SS are responsible for the data acquisition, whereas JL and MM contributed most. JL is responsible for the data analyses. JL prepared the manuscript with contributions from all co-authors. All the authors contributed to the data interpretation.

Competing interests. The authors declare that they have no conflict of interest.

Acknowledgements. This research was funded by the Doctoral Academy Mountain Knowledge of the University of Graz, project Isotopenuntersuchungen zu Schneeschmelzwässer und daraus resultierender Grundwasserneubildung im Einzugsgebiet der Etzbachquelle und deren Auswirkung auf die Abflusskomponententrennung (EZBQsnowHunt), and the Austrian Academy of Sciences within the ESS project ECOSPRING. The snow sampling at the Bärenkar cirque could not have been successful without the help of colleagues. Therefore, the authors express their gratitude to Jakob Halder for his time and above all energy to help collect the snow samples. We also thank Tereza Kunkelova for her lab work, operating the isotope analyser and providing us the data in an orderly fashion. The authors are grateful for free access to the ERA5 reanalysis data provided by the ECMWF. The authors also thank the Forestry of Styria for access to the research area. The authors acknowledge the usage of Claude Sonnet 4.6 for structure and readability.

https://doi.org/10.5194/egusphere-2026-2190
Preprint. Discussion started: 5 June 2026

References

Aemisegger, F. and Sjölte, J.: A Climatology of Strong Large-Scale Ocean Evaporation Events. Part II: Relevance for the Deuterium Excess Signature of the Evaporation Flux, J. Climate, 31, 7313–7336, https://doi.org/10.1175/JCLI-D-17-0592.1, 2018.

Aemisegger, F., Pfahl, S., Sodemann, H., Lehner, I., Seneviratne, S., and Wernli, H.: Deuterium excess as a proxy for continental moisture recycling and plant transpiration, Atmos. Chem. Phys., 14, 4029–4054, https://doi.org/10.5194/acp-14-4029-2014, 2014.

Aemisegger, F., Trachsel, J., Sadowski, Y., Eichler, A., Lehning, M., Avak, S., and Schneebeli, M.: Fingerprints of Frontal Passages and Post-Depositional Effects in the Stable Water Isotope Signal of Seasonal Alpine Snow, J. Geophys. Res. Atmos., 127, e2022JD037 469, https://doi.org/10.1029/2022JD037469, 2022.

Anderson, L., Berkelhammer, M., and Mast, M.: Isotopes in North American Rocky Mountain Snowpack 1993 - 2014, Quat. Sci. Rev., 131, 262–273, https://doi.org/10.1016/j.quascirev.2015.03.023, 2016.

Barnett, T., Adam, J., and Lettenmaier, D.: Potential impacts of a warming climate on water availability in snow-dominated regions, Nature, 438, 303–309, https://doi.org/10.1038/nature04141, 2005.

Berghuijs, W., Woods, R., and Hrachowitz, M.: A Precipitation Shift from Snow towards Rain Leads to a Decrease in Streamflow, Nat. Clim. Change, 4, 583–586, https://doi.org/10.1038/nclimate2246, 2014.

Beria, H., Larsen, J., Ceperley, N., Michelon, A., Vennemann, T., and Schaefli, B.: Understanding snow Hydrol. Processes through the lens of stable water isotopes, WIREs Water, 5, https://doi.org/10.1002/wat2.1311, 2018.

Bershaw, J.: Controls on Deuterium Excess across Asia, Geosciences, 8, 257, https://doi.org/10.3390/geosciences8070257, 2018.

Birkeland, K.: Terminology and Predominant Processes Associated with the Formation of Weak Layers of Near-Surface Faceted Crystals in the Mountain Snowpack, Arct. Alp. Res., 30, 193–199, https://doi.org/10.1080/00040851.1998.12002891, 1998.

Carroll, R., Deems, J., Niswonger, R., Schumer, R., and Williams, K.: The Importance of Interflow to Groundwater Recharge in a Snowmelt-Dominated Headwater Basin, Geophys. Res. Lett., 46, 5899–5908, https://doi.org/10.1029/2019GL082447, 2019.

Carroll, R., Deems, J., Maxwell, R., Sprenger, M., Brown, W., Newman, A., Beutler, C., Bill, M., Hubbard, S., and Williams, K.: Variability in observed stable water isotopes in snowpack across a mountainous watershed in Colorado, Hydrol. Processes, 36, https://doi.org/10.1002/hyp.14653, 2022.

Colbeck, S.: Theory of metamorphism of dry snow, J. Geophys. Res., 88, 5475–5482, https://doi.org/10.1029/JC088iC09p05475, 1983.

Colbeck, S.: Temperature-dependence of the equilibrium form of ice, J. Cryst. Growth, 72, 726–732, 1985.

Colbeck, S.: A review of the metamorphism and classification of seasonal snow cover crystals, in: Avalanche Formation, Movement and Effects, no. 162 in IAHS Publ., 1987.

Colbeck, S. C.: The layered character of snow covers, Rev. Geophys., 29, 81–96, https://doi.org/10.1029/90rg02351, 1991.

Craig, H.: Isotopic variations in meteoric waters, Science, 133, https://doi.org/10.1126/science.133.3465.1702, 1961.

Craig, H. and Gordon, L.: Deuterium and oxygen 18 variations in the ocean and the marine atmosphere, in: Stable Isotopes in Oceanographic Studies and Paleotemperatures, edited by Tongiorgi, E., pp. 9–130, Consiglio Nazionale delle Ricerche, Pisa, 1965.

Dafflon, B., Wielandt, S., Lamb, J., McClure, P., Shirley, I., Uhlemann, S., Wang, C., Fiolleau, S., Brunetti, C., Akins, F., Fitzpatrick, J., Pullman, S., Busey, R., Ulrich, C., Peterson, J., and Hubbard, S.: A distributed temperature profiling system for vertically and laterally dense acquisition of soil and snow temperature, The Cryosphere, 16, 719–736, https://doi.org/10.5194/tc-16-719-2022, 2022.

Dansgaard, W.: Stable isotopes in precipitation, Tellus, 16, 436–468, https://doi.org/10.1111/j.2153-3490.1964.tb00181.x, 1964.

https://doi.org/10.5194/egusphere-2026-2190
Preprint. Discussion started: 5 June 2026

Delattre, H., Valet-Coulomb, C., and Sonzogni, C.: Deuterium excess in the atmospheric water vapour of a Mediterranean coastal wetland: regional vs. local signatures, Atmos. Chem. Phys., 15, 10 167–10 181, https://doi.org/10.5194/acp-15-10167-2015, 2015.

Draxler, R. and Hess, G.: An overview of the HYSPLIT4 modelling system for trajectories, dispersion and deposition, Aust. Meteorol. Mag., 47, 295–308, https://doi.org/10.1071/ES98032, 1998.

Dubbert, M. and Werner, C.: Water fluxes mediated by vegetation: emerging isotopic insights at the soil and atmosphere interfaces, New Phytol., 221, 1754–1763, https://doi.org/10.1111/nph.15547, 2018.

Dütsch, M., Pfahl, S., and Sodemann, H.: The Impact of Nonequilibrium and Equilibrium Fractionation on Two Different Deuterium Excess Definitions, J. Geophys. Res. Atmos., 122, 12 732–12 746, https://doi.org/10.1002/2017JD027085, 2017.

Feng, X., Faiia, A., and Posmentier, E.: Seasonality of isotopes in precipitation: A global perspective, J. Geophys. Res. Atmos., 114, https://doi.org/10.1029/2008JD011279, 2009.

Fierz, C., Armstrong, R., Durand, Y., Etchevers, P., Greene, E., McClung, D., Nishimura, K., Satyawali, P., and Sokratov, S.: The International Classification for Seasonal Snow on the Ground, UNESCO, 2009.

Filippa, G., Maggioni, M., Zanini, E., and Freppaz, M.: Analysis of continuous snow temperature profiles from automatic weather stations in Aosta Valley (NW Italy): Uncertainties and applications, Cold Reg. Sci. Technol., 104-105, 54–62, https://doi.org/10.1016/j.coldregions.2014.04.008, 2014.

Fuchsberger, J. and Kirchengast, G.: Release Notes for Version 8.0 of the WegenerNet Processing System (WPS Level 2 data v8), 2023.

Fujita, K. and Abe, O.: Stable isotopes in daily precipitation at Dome Fuji, East Antarctica, Geophys. Res. Lett., 33, https://doi.org/10.1029/2006GL026936, 2006.

Gat, J.: Oxygen and hydrogen isotopes in the hydrologic cycle, Annu. Rev. Earth Planet. Sci., 24, 225–262, https://doi.org/10.1146/annurev.earth.24.1.225, 1996.

Giorgino, T.: Computing and Visualizing Dynamic Time Warping Alignments in R: The dtw Package, J. Stat. Softw., 31, 1–24, https://doi.org/10.18637/jss.v031.i07, 2009.

Graham, R. M., Hudson, S. R., and Maturilli, M.: Improved performance of ERA5 in Arctic Gateway Relative to four global atmospheric reanalyses, Geophys. Res. Lett., 46, 6138–6147, https://doi.org/10.1029/2019gl082781, 2019.

Harris Stuart, R., Faber, A., Wahl, S., Hörhold, M., Kipfstuhl, S., Vasskog, K., Behrens, M., Zuhr, A., and Steen-Larsen, H.: Exploring the role of snow metamorphism on the isotopic composition of the surface snow at EastGRIP, The Cryosphere, 17, 1185–1204, https://doi.org/10.5194/tc-17-1185-2023, 2023.

Hassler, B. and Lauer, A.: Comparison of Reanalysis and Observational Precipitation Datasets Including ERA5 and WFDE5, Atmosphere, 12, 1462, https://doi.org/10.3390/atmos12111462, 2021.

Hersbach, H., Bell, B., Berrisford, P., Hirahara, S., Horányi, A., Muñoz-Sabater, J., Nicolas, J., Peubey, C., Radu, R., Schepers, D., Simmons, A., Soci, C., Abdalla, S., Abellan, X., Balsamo, G., Bechtold, P., Biavati, G., Bidlot, J., Bonavita, M., De Chiara, G., Dahlgren, P., Dee, D., Diamantakis, M., Dragani, R., Flemming, J., Forbes, R., Fuentes, M., Geer, A., Haimberger, L., Healy, S., Hogan, R., Hólm, E., Janisková, M., Keeley, S., Laloyaux, P., Lopez, P., Radnoti, G., de Rosnay, P., Rozum, I., Vamborg, F., Villaume, S., and Thépaut, J.-N.: The ERA5 global reanalysis, Q. J. R. Meteorol. Soc., 146, 1999–2049, https://doi.org/10.1002/qj.3803, 2020.

Huang, J., Yin, J., Wang, M., He, Q., Guo, J., Zhang, J., Liang, X., and Xie, Y.: Evaluation of five reanalysis products with radiosonde observations over the central Taklimakan Desert during summer, Earth Space Sci., 8, e2021EA001 707, https://doi.org/10.1029/2021ea001707, 2021.

https://doi.org/10.5194/egusphere-2026-2190
Preprint. Discussion started: 5 June 2026

Huss, M., Bookhagen, B., Huggel, C., Jacobsen, D., Bradley, R., Clague, J., Vuille, M., Buytaert, W., Cayan, D., Greenwood, G., Mark, B., Milner, A., Weingartner, R., and Winder, M.: Toward mountains without permanent snow and ice, Earth's Future, 5, https://doi.org/10.1002/2016EF000514, 2017.

Jasechko, S.: Global Isotope Hydrogeology - Review, Rev. Geophys., 57, 835–965, https://doi.org/10.1029/2018RG000627, 2019.

Jouzel, J., Alley, R., Cuffey, K., Dansgaard, W., Grootes, P., Hoffmann, G., Johnsen, S., Koster, R., Peel, D., Shuman, C., Stievenard, M., Stuiver, M., and White, J.: Validity of the temperature reconstruction from water isotopes in ice cores, J. Geophys. Res. Oceans, 102, 26 471–26 487, https://doi.org/10.1029/97JC01283, 1997.

Juhlke, T., Meier, C., van Geldern, R., Vanselow, K., Wernicke, J., Baidulloeva, J., Barth, J., and Weise, S.: Assessing moisture sources of precipitation in the Western Pamir Mountains (Tajikistan, Central Asia) using deuterium excess, Tellus B, 71, https://doi.org/10.1080/16000889.2019.1601987, 2019.

Kendall, C. and McDonnell, J.: Isotope Tracers in Catchment Hydrology, Elsevier, 1998.

Kern, Z., Kohán, B., and Leuenberger, M.: Precipitation isoscape of high reliefs: interpolation scheme designed and tested for monthly resolved precipitation oxygen isotope records of an Alpine domain, Atmos. Chem. Phys., 14, 1897–1907, https://doi.org/10.5194/acp-14-1897-2014, 2014.

Krklec, K., Domínguez-Villar, D., and Lojen, S.: The impact of moisture sources on the oxygen isotope composition of precipitation at a continental site in central Europe, J. Hydrol., 561, 810–821, https://doi.org/10.1016/j.jhydrol.2018.04.045, 2018.

Kulkarni, A., Randhawa, S., Rathore, B., Bahuguna, I., and Sood, R.: Snow and glacier melt runoff model to estimate hydropower potential, J. Indian Soc. Remote Sens., 30, 221–228, https://doi.org/10.1007/BF03000365, 2002.

Lammers, J.: Bärenkar field campaign data 2024 - 2025, https://doi.org/10.4211/hs.cf8ad9c275464c0faaf9fe4a3ada05f7, https://doi.org/10.4211/hs.cf8ad9c275464c0faaf9fe4a3ada05f7, hydroShare [data set], 2025.

Mankin, J., Viviroli, D., Singh, D., Hoekstra, A., and Diffenbaugh, N.: The potential for snow to supply human water demand in the present and future, Environ. Res. Lett., 10, https://doi.org/10.1088/1748-9326/10/11/114016, 2015.

Merlivat, L. and Jouzel, J.: Global Climatic Interpretation of the Deuterium-Oxygen 18 Relationship for Precipitation, J. Geophys. Res., 84, https://doi.org/10.1029/JC084iC08p05029, 1979.

Morstad, B., Adams, E., and McKittrick, L.: Experimental and analytical study of radiation-recrystallized near-surface facets in snow, Cold Reg. Sci. Technol., 47, 90–101, https://doi.org/10.1016/j.coldregions.2006.08.023, 2007.

Musselman, K., Clark, M., Liu, C., Ikeda, K., and Rasmussen, R.: Slower snowmelt in a warmer world, Nat. Clim. Change, 7, https://doi.org/10.1038/nclimate3225, 2017.

Nakamura, T., Abe, O., Hasegawa, T., Tamura, R., and Ohta, T.: Spectral reflectance of snow with a known grain-size distribution in successive metamorphism, Cold Reg. Sci. Technol., 32, 13–26, https://doi.org/10.1016/S0165-232X(01)00019-2, 2001.

Natali, S., Doveri, M., Giannecchini, R., Baneschi, I., and Zanchetta, G.: Is the deuterium excess in precipitation a reliable tracer of moisture sources and water resources fate in the western Mediterranean? New insights from Apuan Alps (Italy), J. Hydrol., 614, https://doi.org/10.1016/j.jhydrol.2022.128497, 2022.

Noor, K., Marttila, H., Klöver, B., Welker, J., and Ala-aho, P.: The Spatiotemporal Variability of Snowpack and Snowmelt Water 18O and 2H Isotopes in a Subarctic Catchment, Water Resour. Res., 59, e2022WR033 101, https://doi.org/10.1029/2022wr033101, 2023.

Ollivier, I., Steen-Larsen, H., Stenni, B., Arnaud, L., Casado, M., Cauquoin, A., Dreossi, G., Genthon, C., Minster, B., Picard, G., Werner, M., and Landais, A.: Surface processes and drivers of the snow water stable isotopic composition at Dome C, East Antarctica - a multi-dataset and modelling analysis, The Cryosphere, 19, 173–200, https://doi.org/10.5194/tc-19-173-2025, 2025.

https://doi.org/10.5194/egusphere-2026-2190
Preprint. Discussion started: 5 June 2026

Pfahl, S. and Sodemann, H.: What controls deuterium excess in global precipitation?, Clim. Past, 10, 771–781, https://doi.org/10.5194/cp-10-771-2014, 2014.

Pinzer, B. and Schneebeli, M.: Snow metamorphism under alternating temperature gradients: Morphology and recrystallization in surface snow, Geophys. Res. Lett., 36, https://doi.org/10.1029/2009GL039618, 2009.

Pinzer, B., Schneebeli, M., and Kaempfer, T.: Vapor flux and recrystallization during dry snow metamorphism under a steady temperature gradient as observed by time-lapse micro-tomography, The Cryosphere, 6, 1141–1155, https://doi.org/10.5194/tc-6-1141-2012, 2012.

Pu, T., Kong, Y., Wang, S., Shi, X., Wang, K., Niu, H., and Chen, P.: Modification of stable isotopes in snow and related post-depositional processes on a temperate glacier of Mt. Yulong, southeast Tibetan Plateau, J. Hydrol., 584, https://doi.org/10.1016/j.jhydrol.2020.124675, 2020.

Rist, A., Roth, L., and Veit, H.: Elevational ground/air thermal gradients in the Swiss inner Alpine Valais, Arct. Antarct. Alp. Res., 52, https://doi.org/10.1080/15230430.2020.1742022, 2020.

Rolland, C.: Spatial and Seasonal Variations of Air Temperature Lapse Rates in Alpine Regions, J. Climate, 16, 1032–1046, https://doi.org/10.1175/1520-0442(2003)016<1032:SASVOA>2.0.CO;2, 2003.

Schindler, F.: Influence of Post-Depositional Processes on the Stable Water Isotopic Composition in Snow and Air, Master's thesis, ETH Zurich, 2020.

Schneebeli, M. and Sokratov, S.: Tomography of temperature gradient metamorphism of snow and associated changes in heat conductivity, Hydrol. Processes, 18, 3655–3665, https://doi.org/10.1002/hyp.5800, 2004.

Sinclair, K. and Marshall, S.: Post-depositional modification of stable water isotopes in winter snowpacks in the Canadian Rocky Mountains, Ann. Glaciol., 49, 96–106, https://doi.org/10.3189/172756408787814979, 2008.

Sodemann, H. and Stohl, A.: Asymmetries in the moisture origin of Antarctic precipitation, Geophys. Res. Lett., 36, https://doi.org/10.1029/2009GL040242, 2009.

Sodemann, H., Schwierz, C., and Wernli, H.: Interannual variability of Greenland winter precipitation sources: Lagrangian moisture diagnostic and North Atlantic Oscillation influence, J. Geophys. Res., 113, https://doi.org/10.1029/2007JD008503, 2008.

Sokratov, S. and Golubev, V.: Snow isotopic content change by sublimation, J. Glaciol., 55, 823–828, https://doi.org/10.3189/002214309790152456, 2009.

Sprenger, M., Lestert, H., Gimbel, K., and Weiler, M.: Illuminating Hydrol. Processes at the soil-vegetation-atmosphere interface with water stable isotopes, Rev. Geophys., 54, 674–704, https://doi.org/10.1002/2015RG000515, 2016.

Steen-Larsen, H., Sveinbjörnsdottir, A., Peters, A., Masson-Delmotte, V., Guishard, M., Hsiao, G., Jouzel, J., Noone, D., Warren, J., and White, J.: Climatic controls on water vapor deuterium excess in the marine boundary layer of the North Atlantic based on 500 days of in situ, continuous measurements, Atmos. Chem. Phys., 14, 7741–7756, https://doi.org/10.5194/acp-14-7741-2014, 2014.

Stenni, B., Scarchilli, C., Masson-Delmotte, V., Schlosser, E., Ciardini, V., Dreossi, G., Grigioni, P., Bonazza, M., Cagnati, A., Karlicek, D., Risi, C., Udisti, R., and Valt, M.: Three-year monitoring of stable isotopes of precipitation at Concordia Station, East Antarctica, The Cryosphere, 10, 2415–2428, https://doi.org/10.5194/tc-10-2415-2016, 2016.

Stewart, I.: Changes in snowpack and snowmelt runoff for key mountain regions, Hydrol. Processes, 23, 78–94, https://doi.org/10.1002/hyp.7128, 2008.

Stichler, W. and Schotterer, U.: From accumulation to discharge: modification of stable isotopes during glacial and post-glacial processes, Hydrol. Processes, 14, 1423–1438, 2000.

https://doi.org/10.5194/egusphere-2026-2190
Preprint. Discussion started: 5 June 2026

Touzeau, A., Landais, A., Morin, S., Arnaud, L., and Picard, G.: Numerical experiments on vapor diffusion in polar snow and firn and its impact on isotopes using the multi-layer energy balance model Crocus in SURFEX v8.0, Geosci. Model Dev., 11, 2393–2418, https://doi.org/10.5194/gmd-11-2393-2018, 2018.

Uemura, R., Matsui, Y., Yoshimura, K., Motoyama, H., and Yoshida, N.: Evidence of deuterium excess in water vapor as an indicator of ocean surface conditions, J. Geophys. Res. Atmos., 113, https://doi.org/10.1029/2008JD010209, 2008.

Viviroli, D., Dürr, H., Messerli, B., Meybeck, M., and Weingartner, R.: Mountains of the world, water towers for humanity: Typology, mapping, and global significance, Water Resour. Res., 43, https://doi.org/10.1029/2006WR005653, 2007.

Wagner, T., Themeßl, M., Schüppel, A., Gobiet, A., H, S., and Birk, S.: Impacts of climate change on stream flow and hydro power generation in the Alpine region, Environ. Earth Sci., 76, https://doi.org/10.1007/s12665-016-6318-6, 2017.

Wahl, S., Walter, B., Aemisegger, F., Bianchi, L., and Lehning, M.: Identifying airborne snow metamorphism with stable water isotopes, The Cryosphere, 18, 4493–4515, https://doi.org/10.5194/tc-18-4493-2024, 2024.

WAIS Divide Project Members: Onset of deglacial warming in West Antarctica driven by local orbital forcing, Nature, 500, 440–444, https://doi.org/10.1038/nature12376, 2013.

Zhu, L., Fan, M., Hough, B., and Li, L.: Spatiotemporal distribution of river water stable isotope compositions and variability of lapse rate in the central Rocky Mountains: Controlling factors and implications for paleoelevation reconstruction, Earth Planet. Sci. Lett., 496, 215–226, https://doi.org/10.1016/j.epsl.2018.05.047, 2018.